Synchrotron radiation study of $Cd_{1-x}Mn_xTe$ ($0 \leq x \leq 0.65$)

M. Taniguchi,* L. Ley, R. L. Johnson, J. Ghijsen, and M. Cardona
Max-Planck-Institut für Festkörperforschung, Heisenbergstrasse 1, D-7000 Stuttgart 80, Federal Republic of Germany
(Received 5 August 1985)

The electronic structure of $Cd_{1-x}Mn_xTe$ ($0 \leq x \leq 0.65$) has been investigated by photoemission in the photon energy range from 20 to 140 eV. A sharp (≈ 1 eV full width at half maximum) peak located 3.4 eV below the valence-band maximum (VBM) is assigned to emission from Mn $3d_\uparrow$ states with e symmetry. The t_2 components hybridize significantly with the Te $5p$ states and contribute therefore nearly uniformly to the top 6 eV of the valence bands. Weak structures below 6 eV of mixed Mn $3d$–Te $5p$ character occur also due to the p-d hybridization. Cd and Te $4d$ core-level binding energies remain constant over the whole range of Mn concentrations when measured relative to the VBM. This implies that there are negligible chemical shifts and that the VBM is not affected by the replacement of Cd by Mn. The increase in the optical gap with x is thus due to an increase of the conduction-band energy, in agreement with a shift in the Te $4d$ absorption threshold as measured by partial-yield spectroscopy. A maximum of the Te $5p$ component in the density of empty conduction states is identified ≈ 2 eV above threshold. The Mn $3p \rightarrow 3d_\downarrow$ excitations are atomiclike. The results are interpreted in terms of a schematic linear-combination-of-atomic-orbitals level scheme for the band structure of $Cd_{1-x}Mn_xTe$.

I. INTRODUCTION

$Cd_{1-x}Mn_xTe$ mixed crystals are substitutional solid solutions in which Mn atoms replace Cd atoms in the fcc sublattice of the zinc blende structure of pure CdTe for Mn concentrations below $x = 0.7$.[1] $Cd_{1-x}Mn_xTe$ belongs to a group of materials referred to as "semimagnetic semiconductors." The magnetic properties are determined by the high magnetic moment of the $3d^5$ (^6S) configuration of the Mn^{2+} ions (4.92 Bohr magnetons). Depending on the Mn concentration three different magnetic phases have been identified in $Cd_{1-x}Mn_xTe$ that result from the antiferromagnetic coupling between spins on neighboring Mn ions.[2,3] The exchange interaction between the Mn $3d$ spin and the valence and conduction electrons leads to a number of magneto-optical effects such as a giant Faraday rotation[1,4] and the splitting of the E_0 exciton in a magnetic field.[5] Aside from the influence of the unfilled Mn $3d$ shell the CdMnTe system exhibits the "standard" properties of a mixed crystal: variation of the energy gaps and the phonon spectrum as a function of alloy composition that are both well understood.[6,7] The fundamental gap of CdTe (E_0), for example, that separates the valence-band maximum at Γ (Γ_8) from the conduction-band minimum (Γ_6) increases linearly at 300 K from 1.53 eV ($x = 0$) to 2.5 eV ($x = 0.7$),[6,8] a situation analogous to that found in nonmagnetic $Cd_{1-x}Zn_xTe$.[9] Crucial information about the energy of the Mn $3d$ levels, their width, and their degree of hybridization with the s-p bands, is still lacking. Two weak absorption bands at 2.4 and 2.6 eV, that are exposed below the onset of the strong E_0 transition for $x \geq 0.6$,[10] have been assigned to spin-flip excitations within the Mn $3d^5$ manifold;[10–13] however, charge transfer transitions from the valence-band maximum (VBM, primarily Te $5p$ states) into empty Mn $3d_\downarrow$ states have also been considered as the origin of these bands.[14,15]

Vecchi *et al.*, on the basis of photoluminescence data, place the Mn $3d^5$ ^6S ground state 0.8 eV below the valence-band maximum.[16] Attempts to localize the $3d$ levels by photoemission have lead to contradicting results. Webb *et al.*[17] and Sobczak *et al.*[18] deduce a value of ≈ 3.5 eV for the binding energy of the Mn $3d$ levels based on subtle changes in the valence-band spectra of CdTe upon alloying with Mn, whereas Orlowski places the same states 7 eV below the VBM.[19] Oelhafen *et al.*,[20] on the contrary, claim that the Mn $3d$ electrons are completely delocalized through hybridization with the s-p valence bands because they produce no discernible features in their angle-resolved photoemission spectra.

In this paper we report the unambiguous identification of Mn $3d$ states in $Cd_{1-x}Mn_xTe$ by photoemission using synchrotron radiation. A Mn $3d$ band, containing about two d electrons per Mn atom, is observed as an intense and sharp peak 3.4 eV below the valence-band maximum for $0.2 \leq x \leq 0.65$ whereas the remainder of the d electrons contributes to the top 8 eV of the valence bands. This information is augmented by core-level spectra and partial-yield spectra in the Te $4d$ and Mn $3p$ core excitation region. The latter provide information about the partial density of conduction states and localized excitations on the Mn ions, respectively. We shall discuss our findings in terms of a simple tight-binding level scheme that reproduces the main features of available band-structure calculations.

II. EXPERIMENTAL

The present experiments were performed on the Flipper II beamline using synchrotron radiation from the DORIS storage ring in Hamburg. A double-pass cylindrical mirror analyzer and a high-resolution plane-grating monochromator were used to obtain angle-integrated photo-

emission spectra. The samples were undoped single crystals grown by a modified Bridgman method with Mn concentrations of 0, 0.2, 0.45, and 0.65, respectively. The compositions have been checked by measuring the lattice constants.[8] The clean surfaces for photoemission measurements were prepared *in situ* by cleavage or scraping under ultrahigh vacuum ($< 2 \times 10^{-10}$ mbar).

III. RESULTS

A. Valence bands

The identification of the Mn $3d$ states is considerably facilitated by the use of tunable synchrotron radiation because the photoemission cross section of Mn $3d$ electrons increases with photon energy, $\hbar\omega$, relative to that of the Cd and Te $5s$ and $5p$ states for photon energies below ~ 100 eV.[21] In Fig. 1 we compare valence-band spectra of $Cd_{0.35}Mn_{0.65}Te$ with those of pure CdTe for excitation energies between 22 and 90 eV. The two sets of spectra differ by an additional peak located 3.4 eV below the valence-band maximum in $Cd_{0.35}Mn_{0.65}Te$. The intensity of the peak increases with $\hbar\omega$ relative to the remainder of the valence-band spectrum and we assign it therefore to emission from Mn $3d$ states. The binding energy of these states is independent of the Mn concentration as illustrated in Fig. 2. We estimate the width [full width at half maximum (FWHM)] of the symmetrical Mn $3d$ peak to be $\approx$ 1 eV from the 90-eV spectrum of Fig. 1. A second, weaker set of structures that is not observed in pure CdTe is seen between 6- and 8-eV binding energy. It is related to the presence of Mn but since it does not show the pronounced enhancement with photon energy relative to the remainder of the valence bands as the 3.4-eV peak it must be of mixed atomic origin.

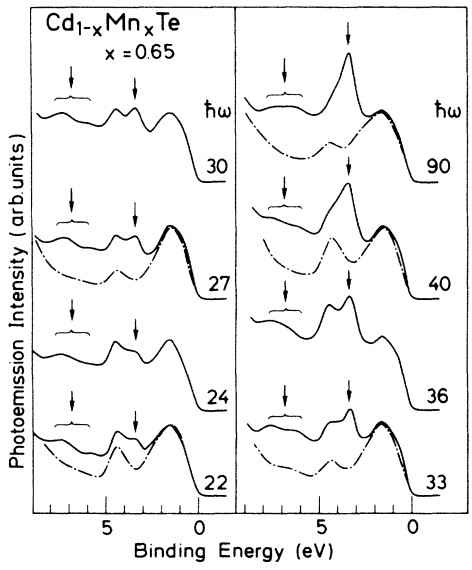

FIG. 1. Valence-band spectra of CdTe (dashed lines) and $Cd_{0.35}Mn_{0.65}Te$ for photon energies between 22 and 90 eV. Mn-induced features are marked by arrows.

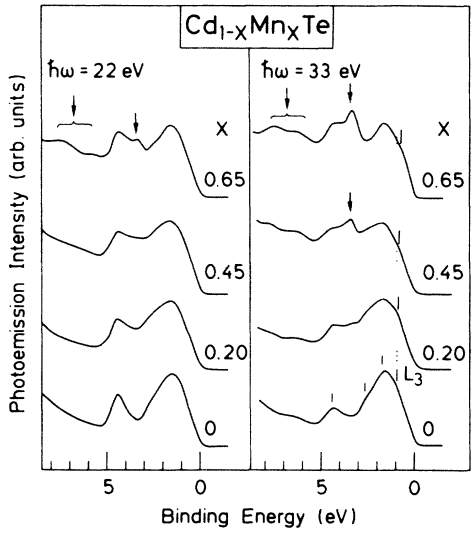

FIG. 2. Valence-band spectra of $Cd_{1-x}Mn_xTe$ for different Mn concentrations. Arrows mark Mn-induced features and vertical marks indicate the position of critical points.

The valence-band spectrum of pure CdTe has been discussed in detail elsewhere.[22] We recall that the two broad peaks reflect maxima in the density of states (DOS) that are primarily derived from Te $5p$ states with an increasing contribution from Cd $5s$ states towards higher binding energy. An almost pure Te $5s$ band is hidden under the Cd $4d$ core-level emission at ≈ 10.3 eV below the VBM (not shown in Figs. 1 and 2).[22] Fine structure in the 33-eV spectrum of Fig. 2 (indicated by vertical marks) is due to the L_3 (0.9 eV), X_5 (1.8 eV), $W_2 - \Sigma_1^{\min}$ (2.7 eV), and L_1 (4.4 eV) Van Hove singularities in the band structure of CdTe.[23] Aside from a blurring of the fine structure, there is no discernible change in the *shape* of the s-p part of the valence-band spectra when Mn is added except for a small shift in the L_3 shoulder from 0.9 eV ($x = 0$) to 0.7 eV ($x = 0.65$) (cf. Fig. 2).

There is, however, a strong Mn $3d$ admixture to these states in $Cd_{1-x}Mn_xTe$ that is best seen when we plot the intensity of the first maximum at 1.5 eV versus photon energy using the emission amplitude of the nearby Cd $4d$ core levels as a reference. This is done for CdTe and $Cd_{0.35}Mn_{0.65}Te$ in Fig. 3(a). The characteristic shape of the relative VB intensity in CdTe is due to a monotonically falling Te $5p$ cross section and a Cd $4d$ photoemission cross section that has a maximum around 50-eV photon energy. In fact, the values of I(1.5 eV)/I(Cd $4d$) can be reproduced to within 50% using calculated photoemission cross sections for the $5p$ and $4d$ shells of Sb and In, respectively, the elements that are next to Te and Cd in the Periodic Table.[21] For this comparison we assumed that the top 6 eV of the VB DOS comprises six electrons of pure Te $5p$ origin.

In $Cd_{0.35}Mn_{0.65}Te$ the relative VB intensity exceeds that found in CdTe for photon energies above 90 eV and reaches an intensity that is 5 times higher than that in the

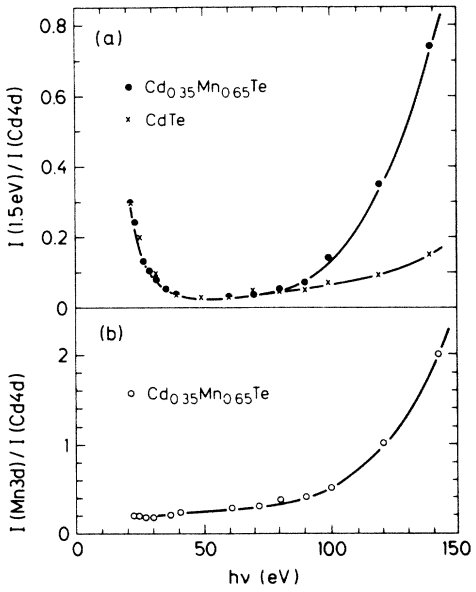

FIG. 3. Normalized amplitudes of (a) the valence band at 1.5 eV, $I(1.5)/I(\text{Cd } 4d)$, and (b) the 3.4-eV Mn peak, $I(\text{Mn } 3d)/I(\text{Cd } 4d)$, as a function of photon energy. The data points for $Cd_{0.35}Mn_{0.65}Te$ in (a) have been corrected for the reduced Cd concentration.

pure compound at $\hbar\omega = 140$ eV. We attribute this additional intensity to the Mn $3d$ admixture because it coincides with the tenfold increase in the relative Mn $3d$ photoemission cross section as documented in Fig. 3(b). Here, we have plotted the amplitude of the peak at 3.4-eV binding energy in $Cd_{0.35}Mn_{0.65}Te$ versus $\hbar\omega$, again using the Cd $4d$ emission for normalization purposes. An estimate of the number of Mn $3d$ electrons necessary to account for the data of Fig. 3(a) can be made as follows.

First we treat the 3.4-eV peak as if it were of pure Mn origin with two d electrons per Mn atom. That this is a reasonable assumption will be explained in Sec. IV. Secondly, we assume that a fraction of the remaining three Mn $3d$ electrons contributes uniformly in energy to the top 6 eV of the valence bands. This accounts for the fact that the *shape* of the valence-band emission is not substantially changed upon the replacement of Cd by Mn. It follows that the relative amplitudes of Fig. 3 are proportional to the relative areas under the 3.4-eV peak and the total VB emission and we calculate that approximately two $3d$ electrons are needed per Mn atom to account for the extra emission intensity throughout the VB in $Cd_{0.35}Mn_{0.65}Te$. Below $\hbar\omega = 60$ eV this Mn $3d$ admixture contributes no more than 0.03 in the units of Fig. 3(a) to $I(1.5\text{ eV})/I(\text{Cd } 4d)$, a value that is too small to distinguish between the two samples. The remaining $3d$ electron is responsible for the structure between 6 and 8 eV.

B. Core-level spectra

The position of the Cd and Te $4d$ core levels relative to the VBM were found to be independent of the Mn concentration to within the experimental error of ± 0.05 eV. The binding energies are 10.00 and 10.65 eV for the Cd $4d_{5/2}$, $4d_{3/2}$ levels and 39.25 and 40.70 eV for the Te $4d$ doublet, respectively; these values agree well with earlier measurements.[22] Since Cd and Te core levels do not change their separation, chemical shifts must be negligible. Thus, we can use them to plot the Mn $3d$ peak and the valence-band maximum on an absolute scale. This is done in Fig. 4 where we have indicated the energy of the conduction-band minimum by adding the E_0 gap to VBM. It is clear from this figure that the increase in the E_0 gap is due to a rising of the conduction band with increasing x. The valence-band discontinuity at the $CdTe/Cd_{1-x}Mn_xTe$ interface should, therefore, be zero aside from an offset induced by interface dipoles that may form when CdTe and $Cd_{1-x}Mn_xTe$ are brought into contact in a superlattice, for example.[24]

C. Core-absorption spectra

Partial-yield spectra, i.e., the yield of secondary electrons as a function of photon energy, represent the optical absorption spectrum provided the electron escape depth is short compared to the penetration depth of the light. This condition is fullfilled for $Cd_{1-x}Mn_xTe$ in the Te $4d$ and Mn $3p$ core excitation region shown in Fig. 5. Structure due to transitions from the Te $4d$ core levels to the conduction band (CB) are observed in the energy region from 37 to 47 eV. The CdTe sample shows two rather broad peaks in this region at 42.6 and 44.0 eV, respective-

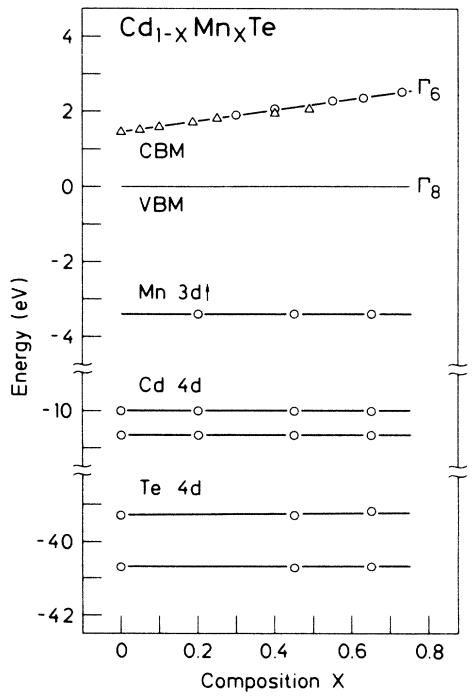

FIG. 4. Experimentally determined energy levels in $Cd_{1-x}Mn_xTe$. The conduction-band minimum (CBM, Γ_6) has been included by adding the E_0 gap to the valence-band maximum (VBM, Γ_8).

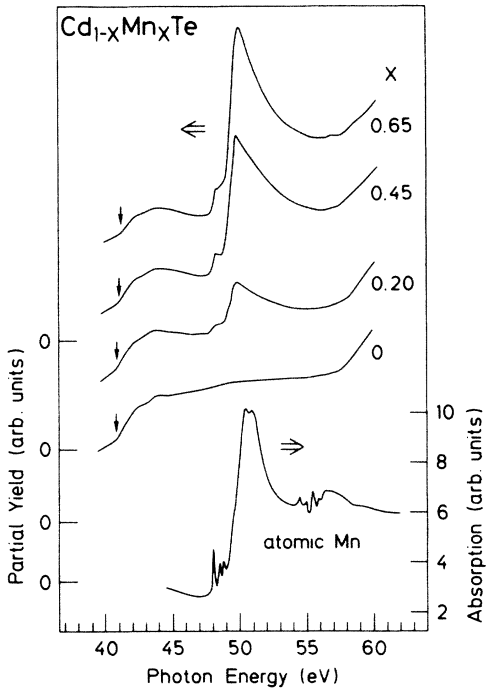

FIG. 5. Partial-yield spectra of $Cd_{1-x}Mn_xTe$ for $x=0$, 0.2, 0.45, and 0.65 in the Te $4d$ and the Mn $3p$ core excitation region (Te, 37–47 eV; Mn, 47–58 eV). The absorption thresholds of the Te $4d$ core spectra are indicated by arrows. The absorption spectrum due to Mn $3p \rightarrow 3d$ transitions in atomic Mn is also shown for comparison (from Ref. 25).

ly, with a splitting that reflects the 1.4-eV spin-orbit splitting of the initial Te $4d$ states. The core-absorption threshold is indicated by an arrow at 40.7 eV. The two peaks are assigned to transitions into maxima of the conduction DOS which lie ~ 2 eV above the conduction-band minimum (CBM) according to the calculations of Chelikowsky and Cohen.[23] These features show little variation with Mn concentration while the threshold shifts from 40.7 ($x=0$) to 41.3 eV ($x=0.65$). The shift is somewhat smaller than the 0.8 eV increase in the E_0 gap between $x=0$ and 0.65.[4–8] The discrepancy may well be due to the poor definition of the threshold. States at the CBM (Γ_6) are of nearly pure Cd-s origin and the core excitations are therefore charge transfer transitions with a small oscillator strength. This fact may also account for the absence of core excitons: the sum of the Te $4d_{5/2}$ binding energy and the E_0 gap equals the core excitation threshold to within 50 meV in CdTe.

While the Te $4d$ absorption spectra are thus well described in terms of the single-particle band-structure picture, we find that the Mn $3p$ core excitations resemble closely those of atomic Mn.[25] The prominent absorption band at 50 eV is due to a transition from the $3p^6 3d^5 4s^2 ({}^6S)$ ground state of the Mn atom into the $3p^5 3d^6 4s^2 ({}^6P)$ excited state.[26,27] The three small peaks at lower energies, not resolved in the spectra of $Cd_{1-x}Mn_xTe$, correspond to transitions into the ${}^6D$ and ${}^4P$ members of the $3p^5 3d^6$ multiplet, respectively. The ${}^6P$ transition is strongly enhanced by a Fano resonance with the degenerate continuum transition $3p^6 3d^5 4s^2 \rightarrow 3p^6 3d^4 4s^2 \epsilon f$ which is also responsible for its width and the asymmetric line shape.[26] Atomiclike $3p$ absorption spectra are also observed in other Mn compounds.[27] They differ from the spectrum of atomic Mn mainly in the position and shape of the ${}^6P$ resonance. In the Mn halides the resonance is narrower and its maximum shifted up to ~ 52 eV.[27] Here we find a down shift by 0.8 to 49.8 eV which is accompanied by a slight broadening of the high-energy tail compared to atomic Mn. Width and energy of a Fano resonance are related to each other as imaginary and real parts of the interaction self-energy, respectively. The interaction of the ${}^6P$ transition with the continuum lowers the excitation energy by 2.2 eV in free Mn.[25] The greater (smaller) shift in $Cd_{1-x}Mn_xTe$ (Mn halides) is thus consistent with an increase (decrease) of the width of the resonance. A simple explanation of these differences cannot be offered at present because they rest on two electron Coulomb integrals involving the $3p$, $3d$, and continuum wave functions, respectively.[26]

IV. DISCUSSION

The interpretation of the valence-band spectra is complicated by the differences in the spatial extent of the contributing atomic orbitals: extended s and p orbitals and the rather localized $3d$ states of the Mn atoms. The s and p orbitals of Cd and Te give rise to the band structure of CdTe. Its photoemission spectrum, like that of all other semiconductors not containing transition metals, is well described in terms of a one-electron picture. That is, the measured ionization potentials are equated with one-electron eigenvalues as obtained in a band-structure calculation. The basis for this interpretation is the tacit assumption that the many-electron response of the system to the ionization can be lumped into an average relaxation energy that is the same for all states over the width of the valence bands. The magnitude of the relaxation energy does not enter as long as energies in theory and experiment are referenced to a common point, the top of the valence bands, for example.[28] This state of affairs is expected to hold for the s-p portions of the valence bands of $Cd_{1-x}Mn_xTe$ as well.

The strong Coulomb interaction between electrons in the spatially confined $3d$ shell defies in general an independent particle description of the ground and ionized states of the $3d$ transition-metal (TM) ions. It stabilizes the high spin ground states in $Cd_{1-x}Mn_xTe$ and in the TM oxides, for example, and is responsible for the insulating nature of these materials despite their unfilled d shells (Mott insulators). The $3d$ features in the photoemission spectra of the TM oxides have been identified with the crystal-field-split multiplets of the d^{n-1} final-state configurations that bear no simple relationship to the one-electron structure of $3d^n$ ground-state configuration in an octahedral field with its e_g and t_{2g} single-particle levels.[29] In MnO ionization of the $3d^5\ {}^6A_1$ ground state of Mn^{2+} leads to two quintet states (${}^5E$ and ${}^5T_2$) of comparable in-

tensity that are separated by about 2 eV. A similar two-peak spectrum, albeit with reversed order of the E and T_2 multiplet, is expected when the Mn^{2+} ion is placed in the tetrahedral environment of CdTe. This is clearly not what we observe in $Cd_{1-x}Mn_xTe$. We suggest therefore that the 3.4-eV peak corresponds to final states of e symmetry whereas the t_2 states hybridize with the $5p$ states of the neighboring Te atoms and are thus responsible for the intensity increase of the valence-band emission, as depicted in Fig. 3, and also for the additional structure below 6 eV binding energy in the spectra of $Cd_{1-x}Mn_xTe$. This interpretation is in essential agreement with the band-structure calculation of Larson *et al.* for antiferromagnetic MnTe in a hypothetical zinc-blende structure.[30]

A schematic energy diagram in Fig. 6 summarizes the formation of the Mn d bands from atomic levels by including interactions one at a time. The level scheme would apply to an isolated substitutional Mn impurity in CdTe as well as to antiferromagnetic MnTe in a zinc-blende structure since interactions between Mn $3d$ states centered on different cation sites have been neglected.

We start on the right-hand side of Fig. 6 with a level scheme that depicts the formation of the near-gap parts of the valence-band structure of CdTe. Energy levels at selected points of the zinc-blende Brillouin zone have been calculated in the LCAO (linear combination of atomic orbitals) approximation using the free atom energy levels and interaction matrix elements given by Harrison.[31] Spin-orbit splittings are neglected. Te and Cd $5p$ electrons combine to form bonding and antibonding states of Γ_{15}, L_3, and X_5 symmetry. Owing to the large energy difference of the Te and Cd $5p$ orbitals, the bonding combinations that form the top 3 eV of the valence bands have predominantly Te $5p$ character. Similarly, the $5s$ electrons of Cd and Te (not shown in Fig. 6) combine to yield a pair of Γ_1 levels, the antibonding Γ_1 state of mainly Cd $5s$ origin determining the bottom of the conduction bands.[32] The remainder of the valence bands are due to mixed s-p hybridization and are not shown in Fig. 6. The experimental valence-band spectrum of CdTe that includes these bands is, however, depicted in the center of Fig. 6 for reference.

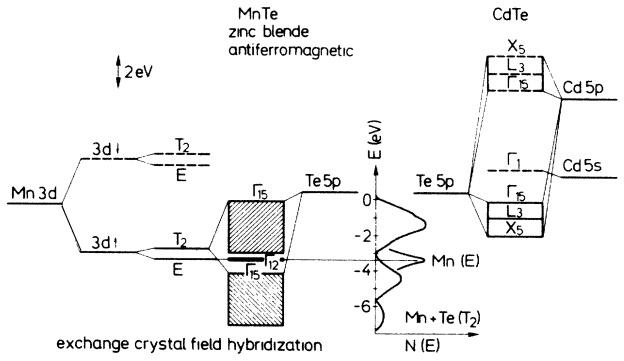

FIG. 6. Schematic energy diagram showing how the observed valence-band spectrum of $Cd_{1-x}Mn_xTe$ (center part) can be constructed from the atomic levels by including interactions one at a time.

On the left-hand side of Fig. 6, the degenerate Mn $3d$ levels are split as a result of the intrashell exchange interaction into a filled spin-up ($3d\uparrow$, five electrons) and an empty spin-down ($3d_\downarrow$) manifold. The exchange splitting is the accepted one-electron representation of the spin-flip excitation energy within the correlated d^5 manifold that is also used in band-structure calculations.[30] The center of gravity of the excited quartet states lies 4.11 eV above the sextet ground state in free Mn^{2+} ions[33] and we adopt this value for the exchange splitting in Fig. 6.

Next the $3d_\uparrow$ and $3d_\downarrow$ states are split in the tetrahedral field of the surrounding ions into E doublets and triplets of T_2 symmetry. Typical values for the crystal-field splitting in Mn compounds range from 0.3 to 1.0 eV and we assume an average value of 0.6 eV.[34]

The $5p$ electrons on neighboring Te atoms have T_2 ($\equiv\Gamma_{15}$) symmetry and there is thus no p-d hybridization for the Mn E states on symmetry grounds. In the absence of interactions with more distant neighbors the E ($\equiv\Gamma_{12}$) levels remain therefore dispersionless and we identify them with the sharp peak seen at 3.4 eV in the photoemission spectra of $Cd_{1-x}Mn_xTe$. By the same token, the Mn $T_2(\Gamma_{15})$ levels hybridize significantly with the Te $5p$ states of the same symmetry and thus add the observed Mn $3d$ character to all Te $5p$ derived bands in $Cd_{1-x}Mn_xTe$. For stoichiometric MnTe the situation would be similar to that found in CuI.[35] Two sets of Γ_{15} derived bands are disposed to either side of the unhybridized Γ_{12} level with the lower bands extending beyond the bottom (not counting the Te $4s$ states) of the CdTe valence bands as shown in Fig. 6. This portion is then responsible for the structure seen between 6 and 8 eV in $Cd_{1-x}Mn_xTe$ samples.

The strong $3d$-$5p$ hybridization is due to the near degeneracy of the Mn $3d$ and Te $5p$ atomic levels. Their relative positions have been adjusted in Fig. 6 so that the Γ_{12} level coincides with the 3.4-eV peak because the $3d$ energies given in Ref. 33 are consistently too low. With this ordering the top of the valence bands has the smallest Mn $3d$ admixture, a fact that explains the insensitivity of the valence-band maximum to alloying (cf. Fig. 4). The increase in the E_0 gap with the gradual replacement of Cd through Mn is due to the higher lying Mn $4s$ level compared to Cd $5s$, as was pointed out by Haas and Ehrenreich.[36]

In the preceding paragraphs we tacitly returned to a one-electron description of the photoemission processes from the Mn $3d$ shell after we had disposed of the exchange energy by considering two spin-polarized $3d$ submanifolds. For the T_2 derived states the one-electron approximation is probably justified because the strong hybridization with the itinerant Te $5p$ electrons has relieved them of most of their localized character. The situation is, in principle, different for the Γ_{12} level which remains rather atomiclike. Multiplet structure is, however, absent because the Γ_{12} level contains only one electron in its final state. A nonvanishing Coulomb energy, U, within the Γ_{12} level lowers the ionization energy by the amount U rela-

tive to its single-particle value. Values around 1.5 eV have been obtained for U by Fazzio *et al.* for transition-metal impurities in III-V and II-VI semiconductors.[37]

V. SUMMARY AND CONCLUSIONS

Our photoemission measurements on $Cd_{1-x}Mn_xTe$ and their interpretation in terms of a simple tight-binding scheme place these semimagnetic semiconductors between the magnetic transition-metal oxides and the transition-metal silicides, for example, which are metallic and only weakly magnetic.[38] In the transition-metal oxides the strong intrashell exchange interaction ensures their insulating character (Mott insulators) and excitations from the well-localized $3d$ shell can only be understood taking multiplet effects into account. This is apparently not required for the interpretation of the $3d$ ionization energies in $Cd_{1-x}Mn_xTe$ because strong hybridization with the Te $5p$ states delocalizes part of the $3d$ manifold sufficiently. It is expected that this hybridization will also be important for the interpretation of the optical transitions near 2.3 eV which involve Mn $3d$ states. The p-d hybridization contributes also to the stability of Mn as a replacement of Cd. This hybridization pushes down the occupied states in the lower regions of the valence bands.

ACKNOWLEDGMENTS

We are grateful to R. R. Galazka of the Institute of Physics, Warsaw, Poland, for supplying the samples and H. Kölln for technical support. We thank W. Gebhardt and H. Ehrenreich for many illuminating discussions. One of us (M.T.) would like to thank the Alexander von Humboldt Foundation for financial support. This project was partially financed by the Bundesminister für Forschung und Technologie (BMFT).

*Permanent address: Synchrotron Radiation Laboratory, Institute of Solid State Physics, The University of Tokyo, Tanashi, Tokyo 188, Japan.

[1]R. R. Galazka, in *Physics of Semiconductors,* edited by B. L. H. Wilson (IOP, Bristol, 1979), p. 133.

[2]R. R. Galazka, S. Nagata, and P. H. Keesom, Phys. Rev. B **22**, 3344 (1980).

[3]S. B. Oseroff, R. Calvo, and W. Giriat, Solid State Commun. **35**, 539 (1980).

[4]J. A. Gaj. R. R. Galazka, and N. Nawrocki, Solid State Commun. **25**, 193 (1978).

[5]J. A. Gaj, J. Ginter, and R. R. Galazka, Phys. Status Solidi B **89**, 655 (1978).

[6]See, e.g., P. Lautenschlager, S. Logothetidis, L. Viña, and M. Cardona, Phys. Rev. **32**, 3811 (1985), and references therein.

[7]A. K. Ramdas and S. Rodriguez, in *Novel Materials and Techniques in Condensed Matter,* edited by G. W. Wobtree and P. Vashishta (North-Holland, Amsterdam, 1982), p. 209.

[8]N. Bottka, J. Stankiewicz, and W. Giriat, J. Appl. Phys. **52**, 4189 (1981).

[9]*Landoldt-Börnstein Tables, New Series, Group III,* edited by O. Madelung, M. Schulz, and H. Weiss (Springer, Berlin, 1982), Vol. 17b.

[10]J. P. Laseary, J. Diouri, M. El Amrani, and D. Coquillat, Solid State Commun. **47**, 709 (1983).

[11]N. T. Khoi and J. A. Gaj, Phys. Status Solidi B **83**, K133 (1977).

[12]Y. R. Lee and A. K. Ramdas, Solid State Commun. **51**, 861 (1984).

[13]E. Müller, W. Gebhardt, and W. Rehwald, J. Phys. C **16**, L1141 (1983).

[14]R. A. Abren, W. Giriat, and M. P. Vecchi, Phys. Lett. **85**, 399 (1981).

[15]P. Lemasson, B. L. Wu, R. Triboulet, and J. Gautron, Solid State Commun. **47**, 669 (1983).

[16]M. P. Vecchi, W. Giriat, and L. Videla, Appl. Phys. Lett. **38**, 99 (1981).

[17]C. Webb, M. Kaminska, M. Lichtensteiger, and J. Lagowski, Solid State Commun. **40**, 609 (1981).

[18]E. Sobczak and H. Sommer, Phys. Status Solidi B **112**, K43 (1982).

[19]B. A. Orlowski, Phys. Status Solidi B **95**, K31 (1979).

[20]P. Oelhafen, M. P. Vecchi, J. L. Freeouf, and V. L. Moruzzi, Solid State Commun. **44**, 1547 (1982).

[21]S. M. Goldberg, C. S. Fadley, and S. Kono, J. Electron Spectrosc. Relat. Phenom. **21**, 285 (1981).

[22]L. Ley, R. A. Pollak, F. R. McFeely, S. P. Kowalczyk, and D. A. Shirley, Phys. Rev. B **9**, 600 (1974); N. J. Shevchik, J. Tejeda, and M. Cardona, Phys. Rev. B **9**, 2627 (1974).

[23]J. R. Chelikowsky and M. L. Cohen, Phys. Rev. B **14**, 556 (1976).

[24]See, e.g., X.-C. Zhang, S. -K. Chang, A. V. Nurmikko, L. A. Kolodziejski, R. L. Gemshov, and S. Datta, Phys. Rev. B **31**, 4056 (1985), and references therein.

[25]R. Bruhn, B. Sonntag, and H. W. Wolff, Phys. Lett. **69A**, 9 (1978).

[26]L. C. Davis and L. A. Feldkamp, Phys. Rev. A **17**, 2012 (1978).

[27]S. Nakai, H. Nakamori, A. Tomita, K. Tsutsumi, H. Nakamura, and C. Sugiura, Phys. Rev. B **9**, 1870 (1974).

[28]This approach is an extension of Koopmans's theorem [T. Koopmans, Physica **1**, 104 (1933)] insofar as the passive orbitals are allowed to relax. For more details, see, e.g., L. Ley and M. Cardona, in *Photoemission in Solids,* edited by M. Cardona and L. Ley (Springer, Heidelberg, 1978), Vol. I, pp. 64ff.

[29]D. E. Eastman and J. L. Freeouf, Phys. Rev. Lett. **34**, 395 (1975).

[30]B. E. Larson, K. C. Haas, H. Ehrenreich, and A. E. Carlsson (unpublished).

[31]W. A. Harrison, *Electronic Structure and the Properties of Solids* (Freeman, San Francisco, 1980).

[32]The corresponding matrix element was adjusted to give the correct gap of 1.53 eV in CdTe after allowance was made for a 0.7-eV spin-orbit splitting of the Γ_{15} level at the top of the valence bands.

[33]C. E. Moore, *Atomic Energy Levels* (National Bureau of Standards, Washington, D.C. 1949).

[34]W. Gebhardt (private communication).
[35]A. Goldmann, J. Tejeda, N. J. Shevchik, and M. Cardona, Phys. Rev. B **10**, 4388 (1974).
[36]K. C. Haas and H. Ehrenreich, J. Vac. Sci. Technol. A **1**, 1678 (1983).
[37]A. Fazzio, M. J. Caldas, and A. Zunger, Phys. Rev. B **30**, 3430 (1984).
[38]G. W. Rubloff, Surf. Sci. **132**, 268 (1983).